8th Int. Beam Instrum. Conf. IBIC2019, Malmö, Sweden JACoW Publishing
ISBN: 978-3-95450-204-2 ISSN: 2673-5350 doi:10.18429/JACoW-IBIC2019-WEPP032

BEAM BASED ALIGNMENT OF ELEMENTS AND SOURCE AT THE ESS LOW ENERGY BEAM TRANSPORT LINE

N. Milas*, M. Eshraqi, B. Gålnander, Y. Levinsen, R. Miyamoto, E. Nilsson and D. C. Plostinar
European Spallation Source ERIC, Lund, Sweden

Abstract

The European Spallation Source (ESS), currently under construction in Lund, Sweden, will be the world's most powerful linear accelerator driving a neutron spallation source, with an average power of 5 MW at 2.0 GeV. The first protons were accelerated at the ESS site during the commissioning of the ion source and low energy beam transport (LEBT), that started in September 2018 and ran until July 2019. Misalignments of the elements in the LEBT can have a strong impact on the final current transmission of the low energy part. In this paper, we present a way to isolate and measure tilts of the elements and the initial centroid divergence of the source. We also present initial test measurements for the ESS LEBT and discuss how to extend the method to other facilities.

INTRODUCTION

The low energy beam transport (LEBT) section of the ESS linac was commissioned at ESS between September 2018 and June 2019. This section has two focusing solenoids and two sets of dipole correctors (steerers) and is responsible for transporting and focusing the beam that will be delivered to the following radio frequency quadrupole (RFQ) [1]. It is crucial not only that the beam entering the RFQ has the correct Twiss parameters, but also that it enters centered and with minimum centroid angular component. For the latter, it is necessary that the elements along the LEBT as well the the source extraction point are well aligned. For the solenoids in the LEBT, tilts creates dipole components and thus trajectory excursions. In order to correct the beam trajectory in the best possible way it is necessary to have, in addition to a good model, knowledge of the elements tilts and also of the initial beam conditions at the extraction point. In this work we present a method to isolate angular misalignments for the LEBT solenoids and also a way to estimate the initial beam centroid angles. The presented method uses the readings from a Non-invasive Profile Monitor [2] (NPM), but we will also discuss a possibility to use an Allison Scanner type Emittance Measurement Unit (EMU) to perform the same measurement. Finally, measurements performed during the LEBT commissioning and their comparisons with beam transmission simulations, taking into account the reconstructed errors, will be shown.

METHOD

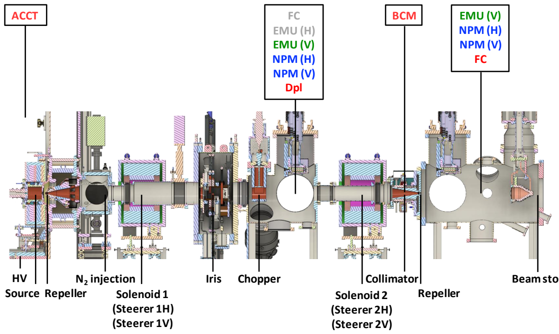

Figure 1: LEBT layout.

In a perfect machine the trajectory should be on the reference axis, however that is seldom the case. Many different errors contribute to offsets in beam trajectory and we face questions of how to identify and make effective estimations of most relevant error sources.For the case of the trajectory in the ESS LEBT (Fig. 1), knowledge of errors in the two solenoids and initial conditions at the source extractions are the keys.

Assuming offsets can be neglected, as assessed in the next section, there are six major error sources to account for: initial centroid angles at the source and tilts around two transverse planes for each solenoid. On the other hand, we have access to only two variables, namely (x, y) positions, at two locations of NPMs downstream of each solenoid. This requires multiple solenoid measurements at different strengths in order to characterize all the six error sources. In this paper, we will use pitch (θ) and yaw (ϕ) as elements tilts, which correspond to a rotation around the vertical and horizontal axis respectively.

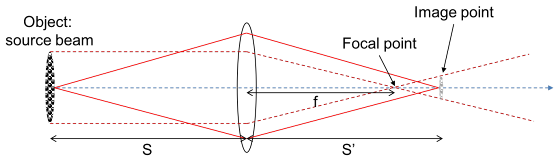

Figure 2: Schematics of the optics of the source and first solenoid at the ESS linac.

The principle of the technique to identify the aforementioned errors, used throughout this paper, is sketched in Fig. 2. When the strength of the solenoid lens is as such to produce the image point at the measurement location, e.g. at the NPM location, the measured position offset is insensitive against the initial errors at the source and dictated by the errors of the solenoid lens itself. In the ESS LEBT, the image point can be easily placed at the first NPM by simply scanning Solenoid 1 strength and finding a value to minimize the beam size at the same NPM. Once this condition is

---

[*] natalia.milas@esss.se

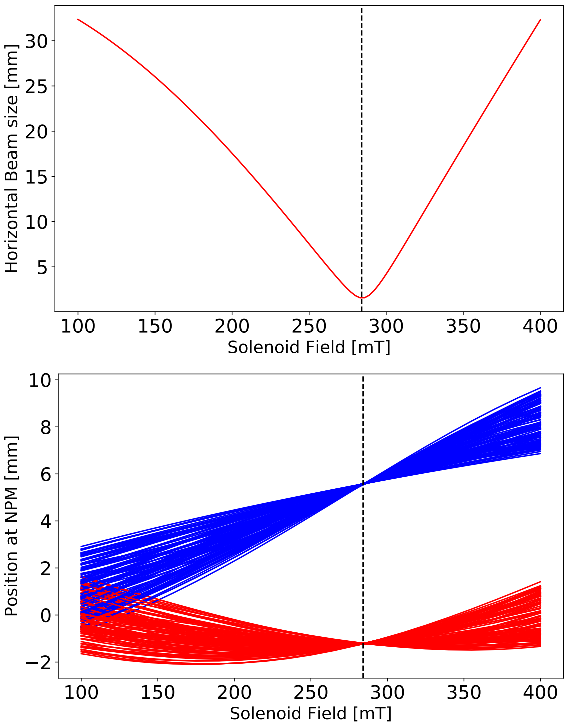

Figure 3: Top: Solenoid focal length scan. The vertical dashed line indicate the focal point. Bottom: 1000 machines simulated varying the sources error and keeping solenoid error fixed, red is horizontal and blue is vertical positions as measured at the NPM. At the image point all lines cross indicating that at that point only solenoid error have an impact on the measured offset.

achieved, the measured position at the NPM ($x_{\mathrm{NPM}}, y_{\mathrm{NPM}}$) and the pitch ($\theta$) and yaw ($\phi$) of Solenoid 1 hold a simple linear relation with a transfer matrix (M), which can be derived for the machine model:

$$\begin{pmatrix} x_{\mathrm{NPM}} \\ y_{\mathrm{NPM}} \end{pmatrix} = M \begin{pmatrix} \theta \\ \phi \end{pmatrix} . \tag{1}$$

Once the tilts for the first solenoid are known from the equation above, it is possible to estimate the initial angles at the source (xp_0, yp_0) too from another linear equation:

$$\begin{pmatrix} x_{\mathrm{NPM}} \\ y_{\mathrm{NPM}} \end{pmatrix} = K \begin{pmatrix} xp_0 \\ yp_0 \end{pmatrix} + \begin{pmatrix} \Delta x \\ \Delta y \end{pmatrix} \tag{2}$$

where the offset term (Δx,Δy) comes from the effects of first solenoid misalignment, calculated on the previous step, and K is another matrix derived again from the model. For the following elements, namely Solenoid 2 for ESS, it is just a matter of iteration of the above process.

SIMULATIONS

This section presents simulations to demonstrate the principle explained in the previous section. Figure 3 (top) shows the beam size scan at the first NPM as a function of Solenoid 1 field. The dashed black line marks the field strength of 284 mT, which minimize the beam size at the first NPM. For this simulation relevant parameters are based on the model described in in [3]. To illustrate that the position offsets at the image point are dictated by the errors of Solenoid 1, 100 different machines were simulated varying the initial angle at the source while keeping the pitch and yaw of Solenoid 1. Figure 3 (bottom) shows the result, and all curves are crossing at a point of the dashed line, as expected.

In the above simulation no linear offsets for the elements or initial beam centroid were included, however they cannot be completely disregarded. A series of statistical analysis was performed to assess the error introduced once offsets and position reading errors are included. In each set 100 machines were simulated and for each simulated machine errors in Solenoid 1, initial centroid angle and Solenoid 2 were reconstructed in this order. For all the set, values of errors in the initial centroid angle and tilts of the two solenoids were maintained. The position reading errors of the NPMs were also kept to 100 µm. In contrast, the values of the offset errors in the initial centroid positions and two solenoids were changed over sets. The distribution used for the offsets was a Unifrom distribution. Table 1 summarizes the results, which shows that method should perform fine even when significant offsets of up to 500 µm are present. As expected the error for the solenoids is independent of the source and other error calculations, thus having both the same spread.

In the studies shown so far the estimation of the initial centroid angles at the source, based on Eq. (2), was performed for a very low solenoid strength of 100 mT. However, a measurement with a very low solenoid strength may be not always trustworthy in a real machine. Figure 4 shows how the error in the reconstruction of the initial centroid angles at the source varies as a function of the solenoid field, assuming a maximum offset of 100 µm. The error is maximized when the image position is at the NPM since there the source effects are minimized and thus more difficult to be accurately measured.

Table 1: Error Analysis as a Function of the Solenoids and Initial Beam Centroid Offsets

Max. Offset	**$\Delta\theta$ and $\Delta\phi$ (mrad)**	**Δxp_0 and Δyp_0 (mrad)**
100 µm	0.2	0.07
200 µm	0.3	0.10
500 µm	0.7	0.15

ESS LEBT MEASUREMENT

During the Ion Source and LEBT commissioning at ESS a series of measurements to assess the beam trajectory in the LEBT were done. In this work we present the measurement data for the latest source configurations with total proton current between 50 and 70 mA extracted from the source [4].

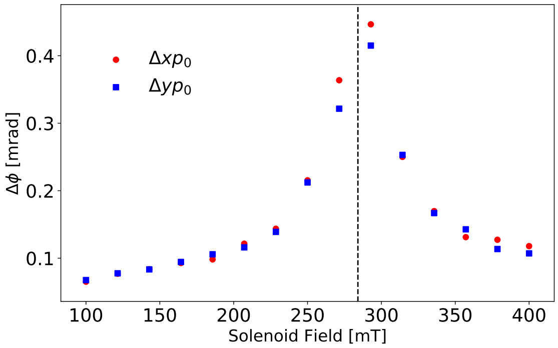

Figure 4: Angular rms error as a function of solenoid field point used to determine the initial source angle. The closer the point is to the image point the bigger the uncertainty in the source initial parameters.

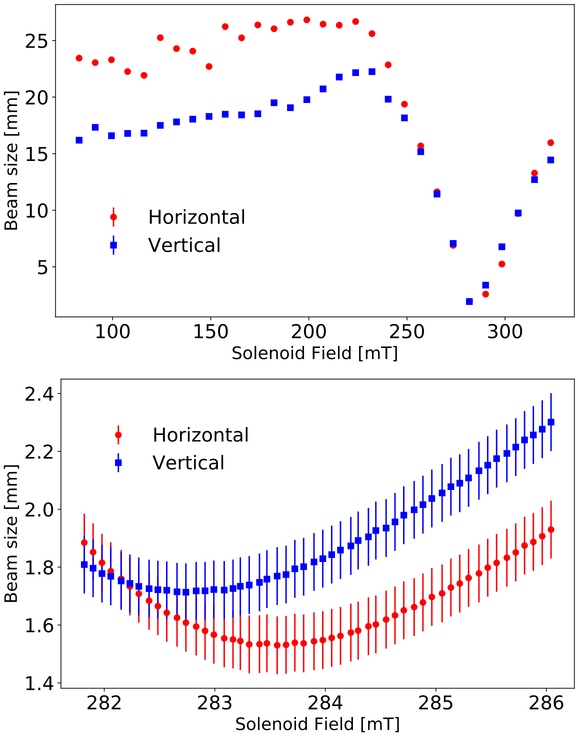

Figure 5: Top: Beam size measured at the first NPM as a function of the Solenoid field. Bottom: Close-up around the image point, or minimum beam size.

The first measurement was to determine the Solenoid 1 field to produce the image point at the first NPM. Figure 5 (top) shows a scan of the beam size as a function of the first solenoid field. As shown, it is possible to determine the image point very accurately, however for solenoid fields too weak or too strong the curves flatten out. This indicates that the beam size is being clipped in some element before the NPM and renders that the measurements are untrustworthy for both beam size and centroid position. This uncertainty also affects the centroid determination since this requires to use a high Solenoid 1 field, which is not ideal for evaluating the initial angles at the source, as shown in Fig. 4.

Figure 5 (bottom) is a more detailed scan around the image point; the solenoid fields to minimize the beam sizes are 283.7 mT for the vertical and 282.7 mT for the horizontal. Table 2 shows a summary of all the measurements of this type during the commissioning and predicted errors for both solenoids and the source. Note, for the solenoid misalignment calculation, average value from both planes was used.

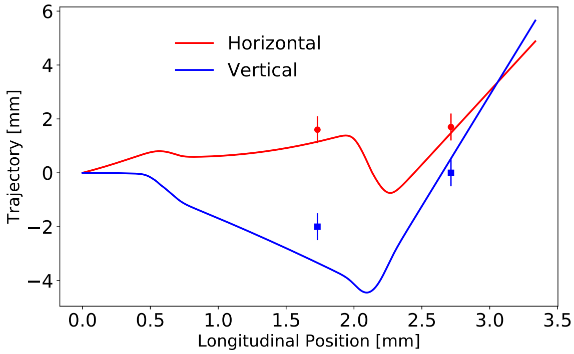

Figure 6: Comparison between the modeled trajectory (lines) and measured positions at both NPMs (markers) in the LEBT.

In order to verify that the predicted solenoid tilts and initial centroid angles at the source reflected the real situation of the machine, a series of simulations were done, as shown in Figs. 6 and 7. For the trajectory simulation the solenoid strengths to maximize transmission, 259.5 mT for Solenoid 1 and 211.4 mT for Solenoid 2, were used. Figure 6 shows the simulated trajectory through the LEBT and commissioning tank, together with the corresponding position measurements at the NPMs. The agreement between model and data is good. Figure 7 shows measured (with a beam current monitor at the RFQ interface) and simulated LEBT output currents for different solenoids strengths, where the simulated data is from particle tracking simulations using TraceWin [5]. Solenoids tilts and initial centroid angle at the source have impacts on the pattern of the output current. Comparing the two cases of simulations without (top right) and with (bottom) taking into account the errors in Table 1 (average over all the measurements), better agreement with the measurements (top left) is visible for the case with the errors, especially for the output current reduction in the region between the week-focusing and strong-focusing regions. On the other hand, the region with high transmissions is still much larger for the simulations, and further improvements might be achieved by using a more realistic initial distribution at the source.

METHOD EXTENSION

Since profile monitors are not the most common diagnostics in the low energy transport part of the majority of machines, an alternative approach for the misalignment measurement, using an EMU, is proposed. In this case the centroid angle error is the important parameters, instead of cen-

Table 2: Measurements Results for Solenoid and Source Misalignments

Date	Solenoid 1 θ (mrad)	 ϕ (mrad)	Source xp_0 (mrad)	 yp_0 (mrad)	Solenoid 2 θ (mrad)	 ϕ (mrad)
16.04.19	−1.1	−3.9	1.2	−0.3	-	-
14.06.19	−0.8	−3.9	1.0	0.2	1.2	10
18.06.19	−1.2	−4.1	1.9	0.0	2.9	7.1
18.06.19	−1.3	−4.2	1.4	0.0	2.3	7.3
18.06.19	−1.4	−4.0	0.9	−0.4	1.4	4.7
02.07.19	−0.0	−5.7	1.2	0.7	-	-
Average	−1.0±0.5	−4.0±0.1	1.3±0.3	0.0±0.4	2.0±0.7	7.0±2.0

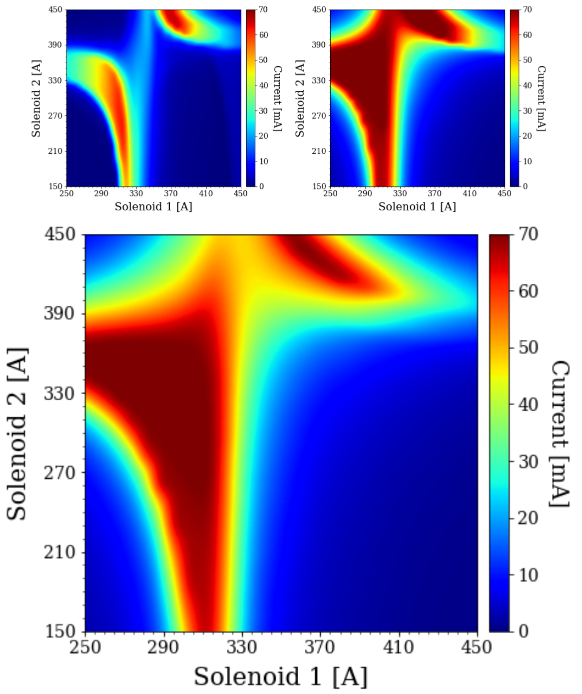

Figure 7: LEBT output current scans. Top left: Measurements from a beam current monitor. Top right: Simulations with no error and default initial values. Bottom: Simulations with errors.

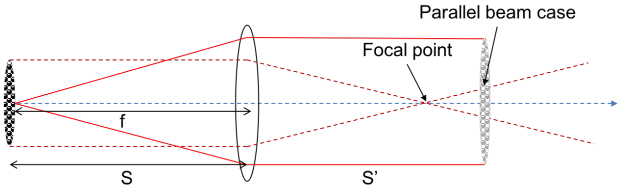

Figure 8: Schematics of the parallel beam condition.

troid position, and the condition of having a parallel beam plays an equivalent role as having the image point at the location of position measurement. The parallel beam can be established by minimizing angular spread, and, once again at this particular solenoid field, only the solenoid errors play roles for the measured beam centroid angle. The relation between the errors and measured parameters is a linear similar to Eq. (1), this time with the angles *xp* and *yp*. Figure 8 shows a schematic of such an optics condition and Fig. 9 shows the crossing of the centroid angles when the parallel beam condition is full-filled.

One drawback of this method with respect to using positions is that a single measurement with the EMU take minutes or longer, while a profile monitor gives instantaneous and continuous data.

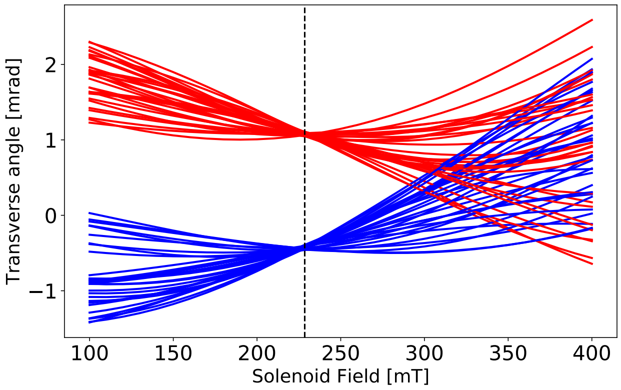

Figure 9: Simulated centroid angles at the EMU location in the LEBT with respect to Solenoid 1 strength, over 100 machines with different errors at the source whereas Solenoid 1 errors being kept. The vertical dashed line indicate the parallel beam condition.

CONCLUSION

The method presented is able to identify the tilts of elements and initial beam angles which are important, in case of low energy beam transport sections, to correct the beam trajectory before transferring it to the next section. For the ESS the next section is the RFQ and knowledge of beam position as well as centroid beam parameters at the entrance are vital to achieve high transmission rate and proper acceleration. This method can also be used in conjunction with EMUs, diagnostics common to many machines and can become a powerful tool in the analysis of the initial sections of hadron linacs

REFERENCES

[1] R. Garoby *et al.*, “The European Spallation Source design”, Phys. Scr., vol. 93, p. 014001, 2018. `doi:10.1088/1402-4896/aa9bff`

[2] C. A. Thomas *et al.*, “Commissioning of the Non-invasive Profile Monitors for the ESS LEBT”, presented at the 8th Int. Beam Instrumentation Conf. (IBIC’19), Malmö, Sweden, Sep. 2019, paper WECO04.

[3] E. Nilsson, M. Eshraqi, J. F. Esteban Müller, Y. Levinsen, N. Milas, and R. Miyamoto, “Beam Dynamics Simulation with an Updated Model for the ESS Ion Source and Low Energy Beam Transport”, in *Proc. 10th Int. Particle Accelerator Conf. (IPAC’19)*, Melbourne, Australia, May 2019, pp. 1042–1045. `doi:10.18429/JACoW-IPAC2019-MOPTS083`

[4] R. Miyamoto *et al.*, “ESS Low Energy Beam Transport Tuning During the First Beam Commissioning Stage”, in *Proc. 10th Int. Particle Accelerator Conf. (IPAC’19)*, Melbourne, Australia, May 2019, pp. 1046–1049. `doi:10.18429/JACoW-IPAC2019-MOPTS084`

[5] D. Uriot and N. Pichoff, “Status of Tracewin Code”, in *Proc. 6th Int. Particle Accelerator Conf. (IPAC’15)*, Richmond, VA, USA, May 2015, pp. 92-94. `doi:10.18429/JACoW-IPAC2015-MOPWA008`